HPGe detectors timing using pulse shape analysis techniques

F.C.L. Crespi [a], V. Vandone [a], S. Brambilla [b], F. Camera [a,*], B. Million [b], S. Riboldi [a], O. Wieland [b]

[a] Dipartimento di Fisica, Università di Milano, Italy
[b] INFN Sezione di Milano, Via Celoria 16, 20133 Milano, Italy

ARTICLE INFO

ABSTRACT

In this work the Pulse Shape Analysis has been used to improve the time resolution of High Purity Germanium (HPGe) detectors. A set of time aligned signals was acquired in a coincidence measurement using a coaxial HPGe and a cerium-doped lanthanum chloride (LaCl$_3$:Ce) scintillation detector. The analysis using a Constant Fraction Discriminator (CFD) time output versus the HPGe signal shape shows that time resolution ranges from 2 to 12 ns depending on the slope in the initial part of the signal. An optimization procedure of the CFD parameters gives the same final time resolution (8 ns) as the one achieved after a correction of the CFD output based on the current pulse maximum position. Finally, an algorithm based on Pulse Shape Analysis was applied to the experimental data and a time resolution between 3 and 4 ns was obtained, corresponding to a 50% improvement as compared with that given by standard CFDs.

© 2010 Elsevier B.V. All rights reserved.

1. Introduction

In-beam gamma spectroscopy is one of the most effective tools for the investigation of nuclear structure. In such experiments, precise time information is extremely important. For instance, it is necessary in heavy-ion fusion-evaporation experiments (to discriminate the unwanted contribution of neutrons by time of flight measurements [1,2]) or in experiments with radioactive ion beams (to suppress the background radiation not coming from the target position [3]).

Next generation gamma spectroscopy arrays like AGATA [4] or GRETA [5] consist of large volume segmented HPGe detectors reconstructing the path of the incident radiation (i.e. gamma-ray tracking). In these detectors, the gamma interaction points are localized with a resolution of at least 5 mm [6–8]. Such position sensitivity is achieved through the segmentation of the outer electrode and the analysis of the charge or current pulse shape (Pulse Shape Analysis, PSA). For this purpose the rising front of the HPGe detector signal is digitized directly at the output of the preamplifier and processed by dedicated real-time PSA algorithms (see [9–19]).

Large volume HPGe detectors have a time resolution limited to about 8–10 ns [20,21]. This is mainly due to the presence of electric noise and the fact that the rising front of the detector signal changes shape depending on the γ-ray interaction positions. The time pick-off algorithm used in most of the in-beam gamma spectroscopy experiments is the Constant Fraction Discriminator (CFD) [20], which starts from the assumption that input signals have a perfectly linear rising front. This is not the case for HPGe.

Such limits in time resolution produce a strong limitation for the use of HPGe detectors in all those cases where time-correlation is more critical than energy resolution. In fact, precise energy resolution and time resolution appear, at the moment, mutually exclusive in the design of gamma detection arrays.

Pulse shape selection methods to improve timing with Ge(Li) detectors were developed in early seventies ([22,23]); in these pioneering works the effectiveness of the method is experimentally demonstrated and a careful study of the dependence of the Ge(Li) detector time resolution on the pulse shape was carried out using analog processing. In the conclusions of these works the importance of the method is clearly pointed out. A successive work [24] showed very interesting and promising results also by using digitized signals. Techniques to extract and improve time information from HPGe signals, alternative to the one presented in this paper, have been also recently discussed both theoretically and with simulated data [25,26]. They have shown very promising results but only on calculated signals and need to be validated in real experimental conditions.

In this work PSA techniques [9,10] have been used to improve a HPGe detector time resolution. The PSA information allowed us to minimize the effects of signal shape variation. The algorithms proposed in this paper have been applied on a set of (time aligned) signals acquired with a coaxial HPGe detector. In this way it was possible to validate and to realistically estimate the time resolution that such techniques can provide.

* Corresponding author.
 E-mail address: camera@mi.infn.it (F. Camera).

A measurement in coincidence mode (using a coaxial HPGe detector and a LaCl$_3$:Ce scintillator) has been performed in order to acquire a set of time aligned signals. This is described in detail in Section 2. In Section 3 the dependence of a standard CFD output on the HPGe signal shape is investigated. In particular it is shown that the optimization procedure of the CFD parameters gives the same final time resolution as the one achieved with the correction of the CFD output depending on the current pulse maximum position without a time consuming optimization of CFD parameters. In Section 4 the results of the PSA algorithm used to extract a time resolution of 3–4 ns are presented and discussed.

2. Measurement of HPGe time aligned signals

This section describes the acquisition procedure of several datasets of time aligned HPGe detector signals, which form the base of the present work.

The experimental setup is displayed in Fig. 1. A ^{60}Co radioactive source (emitting two gamma rays in coincidence, having an energy of 1173 and 1332 keV, respectively) is placed between the front faces of two detectors: a coaxial P-type HPGe (Tennelec model CPVDS30-10195) with 3000 V bias voltage and a LaCl$_3$:Ce crystal, cylindrically shaped, with a diameter of 4″ and 6″ length, coupled to a Photonis XP3540B02 photomultiplier. The signal of both detectors is duplicated. One copy is sent to the digitizer and the other to a CFD module, as sketched in Fig. 1. The trigger of the acquisition is the logic AND between the two CFDs' output and with the LaCl$_3$:Ce CFD signal carrying the time reference. The size of the coincidence window is about 150 ns.

The signal shapes of both detectors have been digitized at 2 GHz in a time window of 1 μs, using a 12 bit CAEN V1729 ADC VME board [27]. The energy threshold of the LaCl$_3$:Ce CFD was set below 1332 keV. In this way only the events in which the lower energy gamma (1173 keV) has interacted in the HPGe detector and the higher energy one (1332 keV) has interacted in the LaCl$_3$:Ce have been selected.

In each coincidence event, the reference time, given by LaCl$_3$:Ce, has been extracted using a digital CFD. The HPGe signals have been consequently aligned in accordance to the time reference given by LaCl$_3$:Ce detector. In this way it was possible

to build a dataset of precisely (i.e. within 1 ns, LaCl$_3$:Ce time resolution) aligned HPGe signals.

3. Time resolution using the CFD algorithm

This section describes the application of the digital CFD algorithm to the measured HPGe signals. Particular attention is devoted to the study of the CFD output dependence on the signal shape. Digital CFD can be described by the formula:

$$Signal\_Out[t_i] = Signal\_In[t_i - d] - F\, Signal\_In[t_i] \qquad (1)$$

The signals have been sampled at 2 GHz: $t_{i+1} - t_i = 0.5$ ns. F is the CFD fraction and d is the CFD shaping delay. The input signal is filtered before applying the CFD, in order to reduce the noise and to eliminate any offset. The filtering consists in a differentiation with a constant f_d followed by an integration with a constant f_i.

In Fig. 2(a) a subset of HPGe signals acquired in the measurement are plotted together with their derivatives (i.e. current pulses, Fig. 2(b)). It can be observed that the position of the current pulse maximum effectively defines the signal shape [9,10]. The dependence of the CFD time output relative to the position of the current maximum is shown in
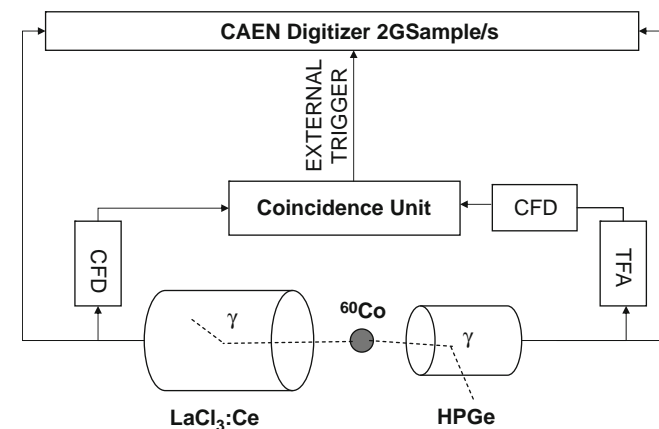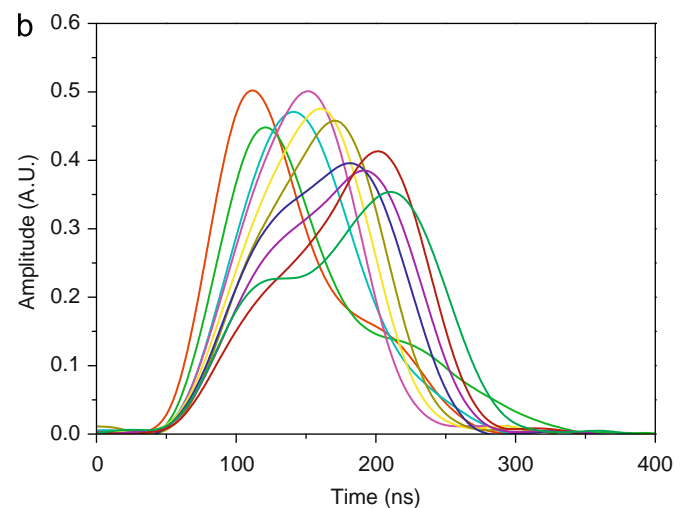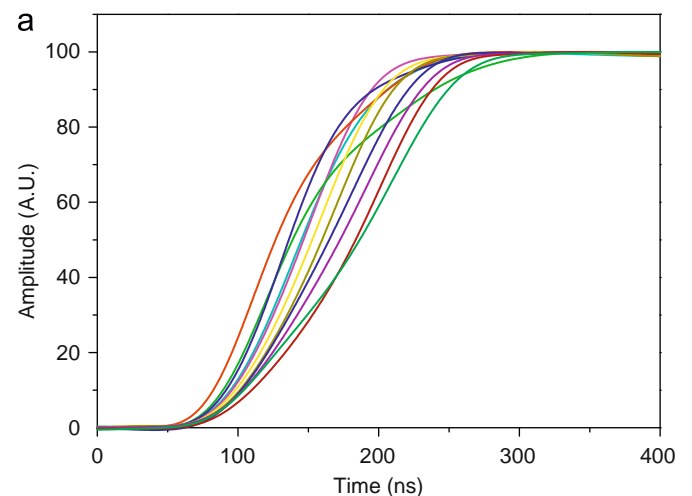

Fig. 2. (a) A selection of the HPGe detector signals acquired in the measurement described in Section 2. The signals have been sampled at the output of the preamplifier with a 2 GHz 12 bits digitizer. (b) The derivative of the signals of Fig. 2(a) is shown.

Fig. 1. Schematic representation of the experimental setup. A ^{60}Co source is placed in front of two detectors: a coaxial HPGe and a LaCl$_3$:Ce scintillator. Both the output signals are duplicated, one is sent to the digitizer and the other to the CFD. The signals coming from HPGe detector have been shaped using a Timing Filter Amplifier placed before the CFD. The acquisition trigger is the logic AND of the two CFDs' output.

Fig. 3. (a) The 2-dimensional histogram displays the CFD output time distribution (y-axis) as a function of the current pulse maximum position (x-axis). (b) The CFD time resolution (i.e. FWHM of the vertical slices of the histogram in Fig. 3(a)) as a function of the current pulse maximum position. In these plots reasonable but unoptimized CFD parameters are used. Error bars are smaller than the size of the symbols.
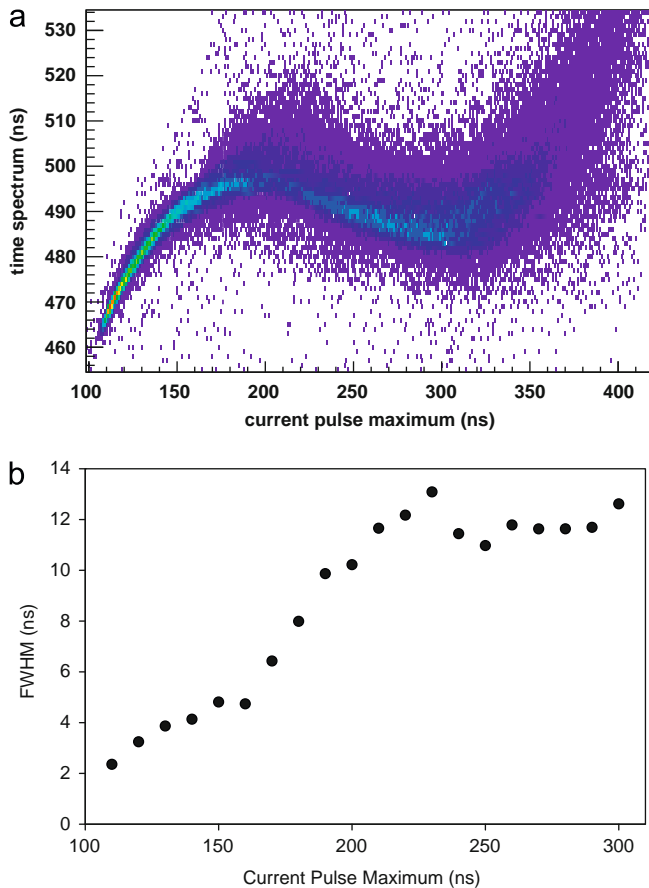
Fig. 4. (a) The 2-dimensional histogram displays the CFD output time distribution (y-axis) as a function of the current pulse maximum position (x-axis). (b) The CFD time resolution (i.e. FWHM of the vertical slices of the histogram in Fig. 4(a)) as a function of the current pulse maximum position. In these plots the CFD parameters values have been selected after an optimization procedure. Error bars are smaller than the size of the symbols.

Fig. 3(a) for $\sim$10 000 acquired events using a reasonable set of CFD parameters ($d=90$ ns; $f_i=150$ MHz; $f_d=5$ MHz; $F=0.25$). In the plot it is evident that not only the centroid of the time distribution but also its FWHM (i.e. the time resolution) changes with the shape of the signals. In Fig. 3(b) the value of the time resolution (FWHM) is plotted as a function of the current pulse maximum position; it is clear that the time resolution is directly proportional to the distance between the signal start and the current pulse maximum. A final time resolution of 14 ns was extracted from the plots (FWHM of the y-axis projection of the 2-D histogram in Fig. 3(a)).

A long and time consuming optimization procedure produced a new set of CFD parameters: $d=34$ ns; $f_i=100$ MHz; $f_d=5$ MHz; $A=0.25$. The optimization procedure involved the use of the CFD algorithm with different sets of parameters, selecting then the combination that minimizes the FWHM of the output time distribution. Fig. 4 displays the plots equivalent to those of Fig. 3 but using the CFD algorithm with the optimized parameters. As can be observed, in this case the dependence of the CFD output on the current pulse maximum position is significantly reduced (i.e. the vertical slices of the 2-dimensional histogram are distributions with aligned centroids). Using the CFD with the optimized coefficients a time distribution with a FWHM of 7.6 ns (black line in histogram in Fig. 6(b)) was obtained.

As the procedure of optimization of the CFD parameters is time consuming and the extracted values might be different for every detector, the data of Fig. 3 (with non-optimized CFD parameters)
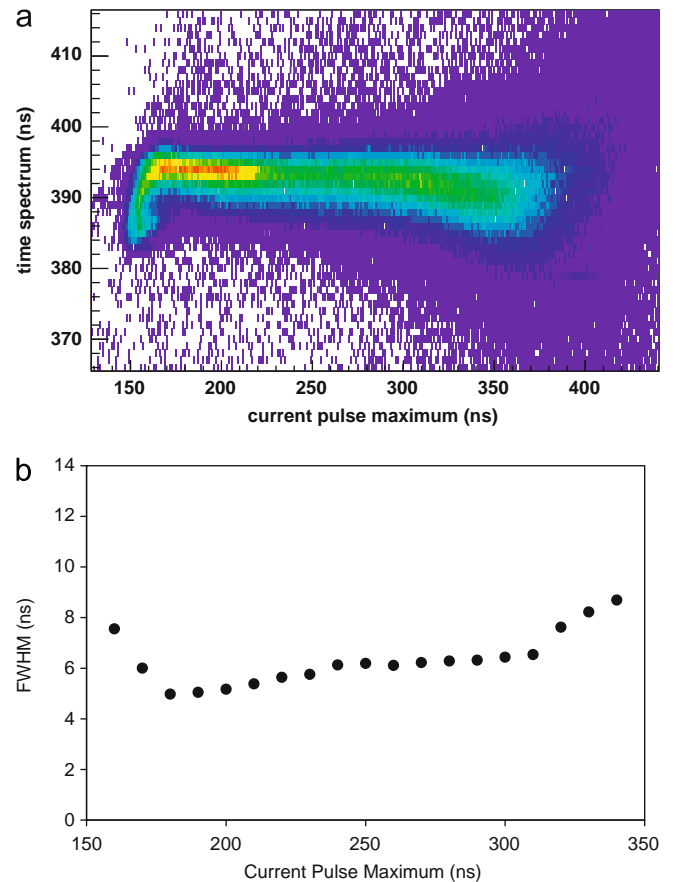
have been aligned on an event by event basis. The alignment algorithm consists in: (i) calculating the position of the current pulse peak for each signal and (ii) correcting with a pre-calculated time shift extracted from Fig. 3(a). Such correction factor is given by the centroid of the time spectra obtained by projecting on the y-axis the proper slice of the 2-D histogram of Fig. 3(a). The slice is the one associated to the current pulse position measured in the step (i). After this procedure a time resolution of $\sim$8 ns (FWHM) has been achieved (grey line histogram in Fig. 6(b)).

The analysis of the previous data has shown that a time resolution of $\sim$8 ns can be achieved either using optimized CFD parameters or aligning the matrix in Fig. 3(a) in the "non-optimized" CFD parameter case. This indicates that the effect of the CFD parameters optimization is to reduce the variation of the output value on the signal shape as much as possible. However, it can be noted from Fig. 4(a) that this dependence was not completely eliminated, especially for the signals with the current pulse maximum positioned in the first part of the rise front ($t_0 < 150$ ns). The comparison between the plots 3b and 4b clearly shows that although the optimization procedure results in an overall time distribution with a smaller FWHM, the same procedure degrades the time resolution of the signals with the shortest rise time.

An additional point that can be observed from Fig. 3(b) is that in the range 100–230 ns, the time resolution is directly proportional to the position of current pulse maximum. In particular, the CFD time resolution ranges from 2 to 12 ns, depending on the
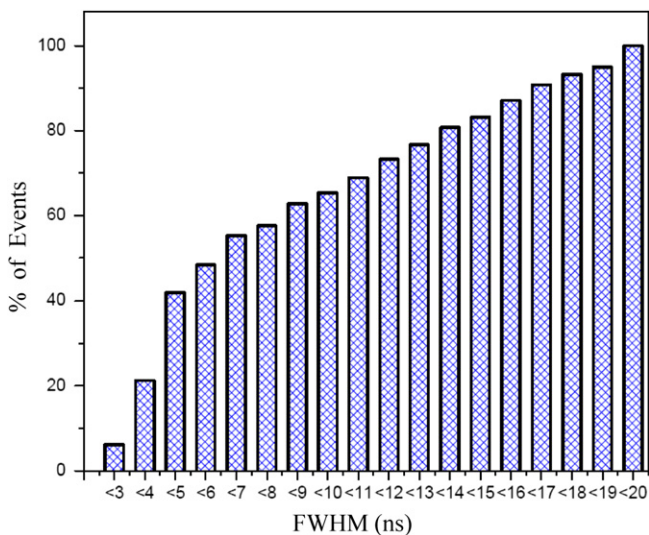
Fig. 5. The histogram shows the percentage of the events with a time resolution below a certain threshold (ns). In this plot the dataset and the CFD parameters of Fig. 3(a) have been used.

slope in the initial part of the signal. This fact is expected since the signal to noise ratio for a time measurement is directly proportional to the derivative of the signal in the point in which the measurement is performed [28].

This fact is extremely interesting since it indicates that it is possible to obtain an extremely good time resolution (2–3 ns) simply using a CFD algorithm with a gate on the shape of the signals, namely on a subset of events of the dataset. In Fig. 5 the percentage of signal shapes (for the case of Fig. 3(a)) with time resolution under a certain threshold is plotted. It can be seen that using 8% of the total events it is possible to achieve a time resolution smaller than 3 ns.

Even if the 8% of events represents a small fraction of all statistics, the possibility of extracting a subset of the data characterized by a scintillator like time resolution (i.e. ∼2–3 ns) could be very useful in in-beam gamma-ray spectroscopy experiments, for example, to better understand the structure of the time spectra and to identify background sources (e.g. gammas coming from ancillary detectors placed near the target, see [3]). This analysis allows setting much more precise time gates, thus extracting spectra with a reduced background.

4. Time resolution using PSA algorithms

This section describes the use of a PSA algorithm to improve HPGe detector time resolution.

The basic idea discussed in this paper is to extract the time information by comparing the detector signal shape with a set of reference signals (signal basis). In gamma-ray tracking with HPGe detectors [4,5] most of the PSA algorithms [9–19] devoted to the spatial localization of the γ-ray interaction points make use of such kind of technique. The basis is usually extracted calculating the induced current pulse shapes by solving the appropriate electrostatic equations ([29,30]), since standard techniques that are used to extract the detector position response experimentally ([31–35]) require an extremely long time for a full-volume detector scan. Although a novel technique that allows a full-volume scan of an HPGe detector to be performed in reasonable time has been recently proposed and validated on a coaxial HPGe

detector [36], it has not yet been experimentally tested on segmented HPGe detectors.

The signal basis used in this work contains all the possible signal shapes produced by the detector following a single interaction event and their time-shifted copies. The level of similarity between two signal shapes is determined using a χ^2 test. The application of the χ^2 test allows finding the signal of the basis that is more similar to the detector signal. If the shape is identical the 2 signals are supposed to have the same time shift, thus the time information needed is just the time-shift of the selected element of the basis.

The experimental extraction of the signal basis has the advantage of avoiding complicated calculations and gives directly the exact response of the detector without any errors introduced by the approximations used in the calculations (e.g. uncertainties in the impurities concentration, cross talk effects or dead layer).

In the case of time information we do not need the association between each element of the basis and a specific position inside the detector. This fact significantly simplifies the procedure for an experimental extraction of the signal basis as compared with the case of γ-ray tracking. Actually one needs only to select a set of signals associated with single interaction events which covers the whole detector volume. The experimental technique used for the production of the signal basis is described in detail in Section 4.1.

For the tests presented in this section, 30 time-shifted copies for each signal have been included in the basis. The relative time shift from one copy to the next is 0.5 ns, thus covering a 15 ns interval. The rationale for the 15 ns time window is that it is possible to easily align all HPGe signals in a time range of 15 ns using a standard CFD.

4.1. Production of the signal basis

The signal basis was built using the experimental data acquired in the measurement described in Section 2. Signals associated with the single interaction events were selected by setting a gate on the Compton edge in the HPGe energy spectrum. These are events in which the 1173 keV gamma ray scattered once in the detector before escaping. Since the localization of the interactions inside the detector is not needed (as in the case of PSA for gamma-ray tracking [9–19]), it is not necessary to know the position associated with each element of the basis. The critical point is that the basis must have a sufficiently large number of events to be sure that all the possible signal shapes are present. The estimation of the number of required events necessary to cover every detector voxel ($\sim$2 mm^3) was done using a GEANT simulation: 3×10^4 events were included in the basis. The 2 GHz sampled signals associated with each event were then down-sampled to 200 MHz. From each of them, 30 time-shifted copies (with a relative time shift of 0.5 ns) are produced, thus covering an interval of 15 ns. These are the elements which constitute the basis ($30 \times 3 \times 10^4$ signals in total).

4.2. Single interaction events

Though the case of a single interaction event represents a very particular situation and covers approximately 40% of the events for a segmented AGATA geometry detector, it is the simplest and easiest for the application of the PSA algorithm. In fact, in this case, the χ^2 comparison between the input signal and the elements of the basis is much faster and simpler than in the case of multiple hit signals.

The χ^2 comparison was applied between signals acquired in the measurement described in Section 2 with the gate on the Compton edge (i.e. single interaction events) and the signal basis.

Two different kinds of time information have been extracted from the χ^2 procedure: (i) the time shift of the element of the basis which minimizes the χ^2 value and (ii) the time shift extracted from the average of the N best fitting signals (N is a free parameter).

The number of signals in the basis is extremely large; in general there is more than one shape for each type which differs only for the statistical fluctuations induced by the electric noise. An averaging procedure reduces the electric noise contribution to time resolution.

It is important to point out that the datasets used to build the time spectra were different from the ones used for the construction of the basis.

In Table 1, the FWHM of the time distribution extracted with the χ^2 comparison procedure of $\sim$7000 signals is reported for different values of the parameter N. It is evident that while for $N=1$ the time resolution is only 9 ns (this is the case in which the time-shift associated with the signal which minimizes the χ^2 was selected) and a significant improvement is achieved for larger values of N. For N larger than 150 time resolution saturates.

Table 1
The values of the FWHM of the time distributions (time resolution) obtained applying the χ^2 comparison procedure described in the text for different values of the parameter N. A single interaction event was selected.

N	FWHM (ns)
1	9.0
5	5.0
10	4.4
15	4.2
20	4.0
30	3.6
45	3.4
60	3.2
150	2.9
200	2.8
300	2.8

An optimal value of $N=60$ was chosen, as a compromise between the time resolution and the amount of computing power needed to process one event. In such configuration a time resolution of 3.2 ns was achieved; Fig. 6(a) shows with a black line histogram the measured time distribution.

4.3. Multiple interaction events

In the case of multiple interaction events, the detector signal is a linear combination of the signals in the basis, weighted by the related deposited energy. As a consequence it is necessary to additionally decompose the input signal into the elements of the basis.

The decomposition algorithm used in this work is the RS algorithm ([9,10]) which performs the following operations:

(i) the position of the maximum of the current pulse is calculated;
(ii) the signal of the basis that better reproduces the input signal around its maximum is selected;
(iii) the selected basis signal is subtracted from the measured one;
(iv) if the decomposed interactions reach an energy weight of 100%, the algorithm stops, otherwise it goes back to step (i). The procedure is repeated up to K times, where K is the maximum number of interactions expected to be present (for the present case a value of $K=2$ has been chosen) in the event.

This problem is exactly the same as that for the localization of the interaction points in γ-ray tracking. As in the single interaction case the basis consists of a dataset of single interaction events and their time-shifted copies. The RS algorithm selects the linear combination of the elements of the basis that best fits the input detector signal and then the time information is determined directly by the time shift of the selected basis signals. Of course all
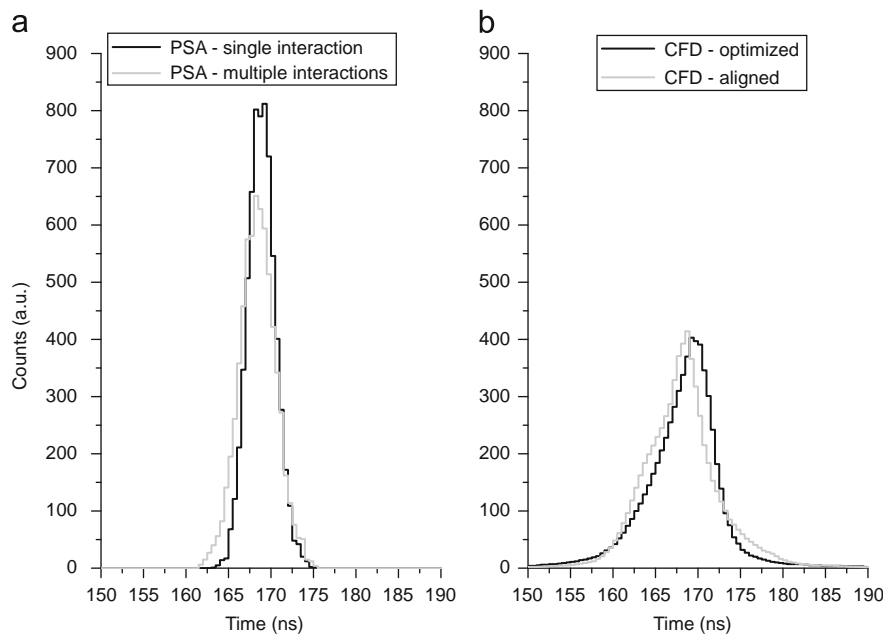

Fig. 6. Right panel: comparison between the time distributions obtained with a standard CFD with optimized coefficients (black line histogram, 7.6 ns FWHM) and the alignment of the centroid positions (grey line histogram, 8.2 ns FWHM; see Section 3 for details). Left Panel: time distributions obtained with the PSA algorithm. The black line histogram (3.2 ns FWHM) is the one related to the single interaction events, and the grey histogram refers to the multiple interaction events (4.2 ns FWHM).

the signals in the linear combination must have the same time shift since different gamma interactions in the same event take place in a time interval of some ps.

The RS algorithm has been applied to a set of $\sim$4500 signals selected with a gate on the 1173 keV full energy peak in the HPGe detector spectrum. In this case there is a very high probability of more than one interaction per event [37,38]. As in the previous section we chose a value of $N=60$. Fig. 6(a) shows, with a grey line histogram, the time spectra obtained applying RS algorithm. A time resolution of 4.2 ns FWHM was obtained.

As expected in this case the time resolution is slightly worse (1 ns) than that achieved with single interaction event signals. This is due to the additional uncertainty introduced by the signal decomposition process. In fact, in some cases, different combinations of the elements of the basis might produce very similar shapes (see Refs. [9,10]).

This value and that of Section 4.2 (i.e. 3.2 ns) must be compared with those of Section 3, obtained using a standard CFD algorithm. The black and grey line histograms in Fig. 6(b) represent the results of a standard CFD with optimized coefficients (black line histogram, 7.6 FWHM) and with the centroid positions alignment (grey line histogram, 8.2 ns FWHM).

All the data analysis has been performed offline as the used codes were not optimized to minimize the execution time. The processor used is an Intel dual core (using one single Xeon 3.2 GHz) and the algorithm code (written in C++) was compiled using the gcc-c++−4.1.2-33 compiler.

5. Conclusions

In this paper, a new method to improve an HPGe detector time resolution by using PSA techniques has been described. The analysis of the time-dependence of the CFD output on the signal shape showed that the time resolution can range from 2 to 12 ns, depending on the slope in the initial part of the signal. It is also shown that the application of an optimization procedure of the CFD parameters gives the same time resolution obtained by performing the correction of the CFD output on the current pulse maximum position, without any CFD parameters optimization procedure. In addition it has been shown that, by selecting a subset of data, a "scintillator like" time resolution of 2–3 ns can be obtained using a standard CFD and exploiting the information of the rise time of the signal on a small subset of events. This fact will be extremely useful in in-beam gamma spectroscopy experiments to understand the structure of the time spectra with high resolution for the optimization of the time gates.

In the case HPGe signals are digitized and stored, an offline analysis using PSA-RS algorithm will permit time resolution of $\sim$4 ns, which is about two times better than that obtained with HPGe arrays using well set standard CFD units.

References

[1] M. Mattiuzzi, et al., Phys. Lett. B 364 (1995) 13.
[2] O. Wieland, et al., Phys. Rev. Lett. 97 (2006) 012501.
[3] H.J. Wollersheim, Nucl. Instr. and Meth. A 537 (2005) 637.
[4] D. Bazzacco, Nucl. Phys. A 746 (2004) 248C;
    J. Gerl, W. Korten (Eds.), AGATA Technical Proposal, September 2001, Available at: ⟨http://www-w2k.gsi.de/agata/⟩.
[5] C.W. Beausang, Nucl. Instr. and Meth. B 204 (2003) 666.
[6] F. Recchia, et al., Nucl. Instr. and Meth. A 604 (2009) 60.
[7] F. Recchia, et al., Nucl. Instr. and Meth. A 604 (2009) 555.
[8] F. Recchia, Ph.D. Thesis, University of Padova, 2008.
[9] F.C.L. Crespi, et al., Nucl. Instr. and Meth. A 570 (2007) 459.
[10] F.C.L. Crespi, et al., Nucl. Instr. and Meth. A 604 (2009) 604.
[11] M. Schlarb, R. Gernhäuser, R. Krücken, in: Simulation and Real-Time Analysis of Pulse Shapes from HPGe Detectors, GSI Scientific Report, 2008 pp. 232.
[12] R. Venturelli, D. Bazzacco, LNL-INFN(REP), 204, 2005, pp. 220.
[13] D.C. Radford, Signal decomposition algorithm for GRETINA, AGATA week GSI 2005. Available at: ⟨http://npg.dl.ac.uk/AGATA/agata_week_talks/⟩.
[14] K. Vetter, et al., Nucl. Phys. A 682 (2001) 286C.
[15] K. Vetter, et al., Nucl. Instr. and Meth. A 452 (2000) 105.
[16] K. Vetter, et al., Nucl. Instr. and Meth. A 452 (2000) 223.
[17] I. Doxas, et al., Nucl. Instr. and Meth. A 580 (2007) 1331.
[18] M. Descovich, et al., Nucl. Instr. and Meth. A 553 (2005) 535.
[19] A. Olariou, P. Desesquelles, et al., IEEE Trans. Nucl. Sci. 53-NS (1, 3) (2006) 1028.
[20] G.F. Knoll, in: Radiation Detection and Measurement, second ed., Wiley, New York, 1989.
[21] L.C. Mihailescu, et al., Nucl. Instr. and Meth. A 578 (2007) 298.
[22] M. Moszynski, B. Bengtson, Application of pulse shape selection method to a true coaxial Ge(Li) detector for measurements of nanosecond half-lives, Nucl. Instr. and Meth. 80 (1970) 233.
[23] B. Bengtson, M. Moszynski, Subnanosecond timng with a planar Ge(Li) detector, Nucl. Instr. and Meth. 100 (1972) 293.
[24] C. Ender, S. Schwebel, C. Ohlemeyer, D. Schwalm, IEEE Nucl. Sci. Symp. Conf. Rec. 1 (1991) 48.
[25] P. Désesquelles et al., J. Phys. G: Nucl. Part. Phys. 36 (3), Article No. 037001.
[26] P. Désesquelles et al., Eur. Phys. J. A 40 (2009) 249–253.
[27] CAEN web page: ⟨http://www.caen.it/⟩.
[28] E. Gatti, et al., Nucl. Instr. and Meth. A 457 (2001) 347.
[29] Th. Kröll, D. Bazzacco, Nucl. Instr. and Meth. A 463 (2001) 227.
[30] P. Medina, et al., in: A Simple Method for the Characterization of HPGe Detectors, IMTC, Como, Italy, 2004.
[31] A. Boston, et al., Nucl. Instr. and Meth. B 261 (2007) 1098.
[32] L. Nelson, et al., Nucl. Instr. and Meth. A 573 (2007) 459.
[33] K. Vetter, et al., Nucl. Instr. and Meth. A 452 (2000) 223.
[34] I. Kojouharov, S. Tashenov, T. Engert, J. Gerl, H. Schaffner, IEEE Nucl. Sci. Symp. Conf. Rec. 3 (2007) 2213.
[35] A. Korichi, M.-H. Ha, presentations at the AGATA week November 12–15, 2007-INFN, Laboratori Nazionali di Legnaro, Italy. AGATA week January 15–19, IPNO and CSNSM laboratories of the IN2P3 institution at the University of Orsay. ⟨http://www-w2k.gsi.de/agata/⟩.
[36] F.C.L. Crespi, Nucl. Instr. and Meth. A 593 (2008) 440.
[37] O. Wieland, et al., Nucl. Instr. and Meth. A 487 (2002) 441.
[38] O. Wieland, et al., IEEE Trans. Nucl. Sci. 48-NS (3) (2001).